J Mater Sci: Mater Med (2009) 20:2337–2347
DOI 10.1007/s10856-009-3792-3

Improved adherence and spreading of Saos-2 cells on polypropylene surfaces achieved by surface texturing and carbon nitride coating

Katja Myllymaa · Sami Myllymaa · Hannu Korhonen · Mikko J. Lammi · Hanna Saarenpää · Mika Suvanto · Tapani A. Pakkanen · Virpi Tiitu · Reijo Lappalainen

Received: 26 February 2009 / Accepted: 21 May 2009 / Published online: 9 June 2009

Abstract The adhesion and contact guidance of human primary osteogenic sarcoma cells (Saos-2) were characterized on smooth, microstructured (MST) and micro- and nano-structured (MNST) polypropylene (PP) and on the same samples with a silicon-doped carbon nitride (C_3N_4-Si) coating. Injection molding was used to pattern the PP surfaces and the coating was obtained by using ultra-short pulsed laser deposition (USPLD). Surfaces were characterized using atomic force microscopy and surface energy components were calculated according to the Owens-Wendt model. The results showed C_3N_4-Si coated surfaces to be significantly more hydrophilic than uncoated ones. In addition, there were 86% more cells in the smooth C_3N_4-Si coated PP compared to smooth uncoated PP and 551%/476% more cells with MST/MNST C_3N_4-Si coated PP than could be obtained with MST/MNST uncoated PP. Thus the adhesion, spreading and contact guidance of osteoblast-like cells was effectively improved by combining surface texturing and deposition of osteocompatible C_3N_4-Si coating.

K. Myllymaa (✉) · S. Myllymaa · H. Korhonen · R. Lappalainen
Department of Physics, University of Kuopio, P.O. Box 1627, 70211 Kuopio, Finland
e-mail: katja.myllymaa@uku.fi

K. Myllymaa
Microsensor Laboratory, School of Engineering and Technology, Savonia University of Applied Sciences, P.O.Box 6, 70201 Kuopio, Finland

M. J. Lammi
Department of Applied Biotechnology, University of Kuopio, P.O. Box 1627, 70211 Kuopio, Finland

M. J. Lammi
Biocenter Kuopio, University of Kuopio, P.O. Box 1627, 70211 Kuopio, Finland

H. Saarenpää · M. Suvanto · T. A. Pakkanen
Department of Chemistry, University of Joensuu, P.O. Box 111, 80101 Joensuu, Finland

V. Tiitu
Department of Biomedicine, Anatomy, University of Kuopio, P.O. Box 1627, 70211 Kuopio, Finland

1 Introduction

The interactions between cells and implants are affected by the surface properties of the implant material. Therefore, several approaches have been introduced to achieve surface modifications to improve cell–biomaterial interactions. The attachment, morphology, proliferation, and function of cells that grow on the surface of the implant are influenced by the size and the shape of the surface features [1–3]. The ability to control cell orientation and morphology through topographical patterning, now referred to as contact guidance, was first observed in the early 1900s [4]. Surface texturing can be achieved in different ways, i.e., by producing surface textures based either on roughness or topography. Surface roughness denotes a random pattern of features usually much smaller than the cell, whereas topography refers to patterns of features placed deliberately on the surface [5]. Many studies have focused on the surfaces textured by various etching and laser micromachining techniques to study the effects of surface topography on cell behaviour [1, 6, 7].

Several different materials have been used as substrates e.g., silicon [7–9], glass [10, 11], and polymers [12–14]. Polymeric substrate materials permit the creation of complex three dimensional shapes the manufacturing of which

with traditional silicon microfabrication techniques would be extremely difficult. In addition the low cost and chemical availability of polymers are advantageous. Previous studies have focused on certain polymers i.e., polystyrene, poly(methylmethacrylate), poly(dimethylsiloxane), and polycarbonate [6], mainly textured using lithographic [15] and soft lithographic [16] techniques.

In the past decade, several methods have been introduced to create polymer surfaces with micro- and nanoscale features [17]. The preparation of structured surfaces with special surface properties such as superhydrophobicity has been a driving force in these studies. One major limitation of most of the methods is the difficulty to control the dimensions of the structures, particularly at the microscale. A new method has been introduced recently where the structural dimensions at the micro- and nano-scales can be simultaneously adjusted. A micro-sized working robot technique and electrochemical treatment of aluminium have been used to make mould inserts which have micro-, nano- or micro-nano dual structures. The molds are used to transfer the structures to plastic surfaces by injection molding. The method is suitable for mass production of surfaces with hierarchical structures [17–20].

Wettability is an important property for an implant material since it plays a crucial role in cell attachment and spreading [21, 22]. If one can enhance the surface wettability, this will increase the surface energy, which is desirable for cell attachment and spreading [Myllymaa et al. unpublished study, 23–25]. The wettability of a solid surface depends on two factors—the surface structure and the surface chemistry. In this study, the contact angles of polypropylene (PP) substrates were decreased by using the Coldab^{TM} ultra-short pulsed laser deposition technique (USPLD) (Picodeon Ltd, Helsinki, Finland) [26]. This technique can be used to produce hybrid thin film coatings in a very well controlled and reproducible manner. Its other advantages are the strong adhesion between coating and substrate material and the possibility to achieve smooth coatings without any additional post treatments.

A novel extremely hard material, carbon nitride (C_3N_4), was theoretically predicted by Liu and Cohen in 1989 [27]. Subsequently, significant efforts were made to verify the bio- and hemocompatible nature of this hard and wear resistance novel material [28–33]. However, the fabrication of CN_x coatings represents a major challenge, even though refinements in the adjustment of the structural, optical, and electronic characteristic are possible. CN_x films have been prepared by ion beam deposition [34], reactive magnetron sputtering [35], dual ion beam sputtering [36], plasma-enhanced chemical vapor deposition [37], and ion implantation [38]. Franco et al. demonstrated how the different experimental parameters of pulsed laser deposition methods (nitrogen pressure, laser fluence, residual atmosphere) can affect the behaviour of the carbon nitride film and noted that the main process parameter determining the nitrogen content of the carbon nitride films is the pressure of the N_2 atmosphere [39].

The surface tension of the carbon films can be modified by incorporating other elements into the carbon matrix to modify the bonding structure. Zhao et al. and Wan et al. demonstrated that silicon-diamond-like carbon (Si-DLC) films with higher Si contents tended to be more hydrophilic and possessed a higher polar component of surface free energy [40, 41]. It has also been suggested that an elevated Si concentration can increase the adsorption of ions onto doped DLC surfaces and that the adsorbed ions cause the surfaces to become more hydrophilic [42]. In our preliminary experiments, we also found C_3N_4-Si film were more hydrophilic compared to pure C_3N_4 one. Other reports have demonstrated the osteocompatibility [43] and hemocompatiblity [44] of Si-DLC films. Si-doped DLC films have also performed better than their pure DLC counterparts in inhibiting bacterial adhesion [40, 45].

The hypothesis tested in this article was that it would be possible to modify adhesion, spreading and contact guidance of osteoblast-like cells by combining microstructuring (MST) and micro- and nano-structuring (MNST) by injection molding with C_3N_4-Si applied by USPLD to PP surfaces. We predicted that the C_3N_4-Si coating would significantly reduce the contact angle of PP surfaces and thus enhance the cell adhesion. We also hypothesized that the increased surface texturing would increase the cell spreading in addition to influencing contact guidance of cells. To test these hypotheses Saos-2 cells were examined in an environmental scanning electron microscope (ESEM) and with MTT assays after a 48 h incubation period.

2 Materials and methods

2.1 Sample fabrication

Electropolished aluminium foils (0.25 mm thick, Puratronic, 99.997%, Alfa Aesar GmbH, Karlsruhe, Germany) were structured with a micro-sized working robot (RP-1AH) made by Mitsubishi Electric Co. (Tokyo, Japan) and equipped with a feedback unit from Delta Enterprise Ltd (Espoo, Finland). Tungsten carbide based tooling tips were supplied by Gritech Ltd (Joensuu, Finland). An anodization process was used to create nanopatterning on the aluminium foils. A more detailed description of micro- and dual-structuring procedures has been reported elsewhere [17–20].

Polypropylene (PP homopolymer, HD 120 MO, Borealis, Porvoo, Finland) sample disks (diameter 25 mm) were injection molded with a DSM (Geleen, The Netherlands)

Midi 2000 extruder − microinjection-molding device. The size of the structured area was 10 × 10 mm^2 as centered. MST samples contained 20 μm high micropillars of diameter of 20 μm. The distance between pillars was also 20 μm. MNST samples had the same microstructure as the MST samples but there was also nanostructuring all over the structured area. The characterization of the structured PP surfaces was undertaken with a Hitachi S4800 FE-SEM instrument (Hitachi High-Technologies Europe GmbH, Krefeld, Germany). Figure 1 shows the SEM images of the structured PP surfaces.

2.2 Laser deposition

The deposition of C_3N_4-Si coatings on PP disc samples was achieved by using ultra-short pulsed laser deposition. Just before deposition, the sample surfaces were gently cleaned using Ar^+ ion sputtering (SAM-7KV, Minsk, Belarus). For USPLD, we used a new type of mode-locked fiber laser (Corelase Ltd, Tampere, Finland) and the Coldab^{TM} deposition technology developed by Picodeon Ltd (Helsinki, Finland) to achieve optimal laser parameters in USPLD [26]. The maximum average power was 20 W at 4 MHz which resulted in a 5 μJ pulse energy. The pulse length was 20 ps. A high purity sintered target of C_3N_4 and Si (10 wt%) was used for deposition. The deposition parameters were adjusted to obtain stable plasma so as to deposit about a 200 nm thick layer. The main aim of depositing C_3N_4-Si was to convert the contact angle of PP surface from being hydrophobic to hydrophilic.

2.3 Samples pretreatment

Samples were cut using a custom-made device with parallel stainless steel blades. Each piece (10 × 10 mm^2) consisted of a single sample texturing and coating material.

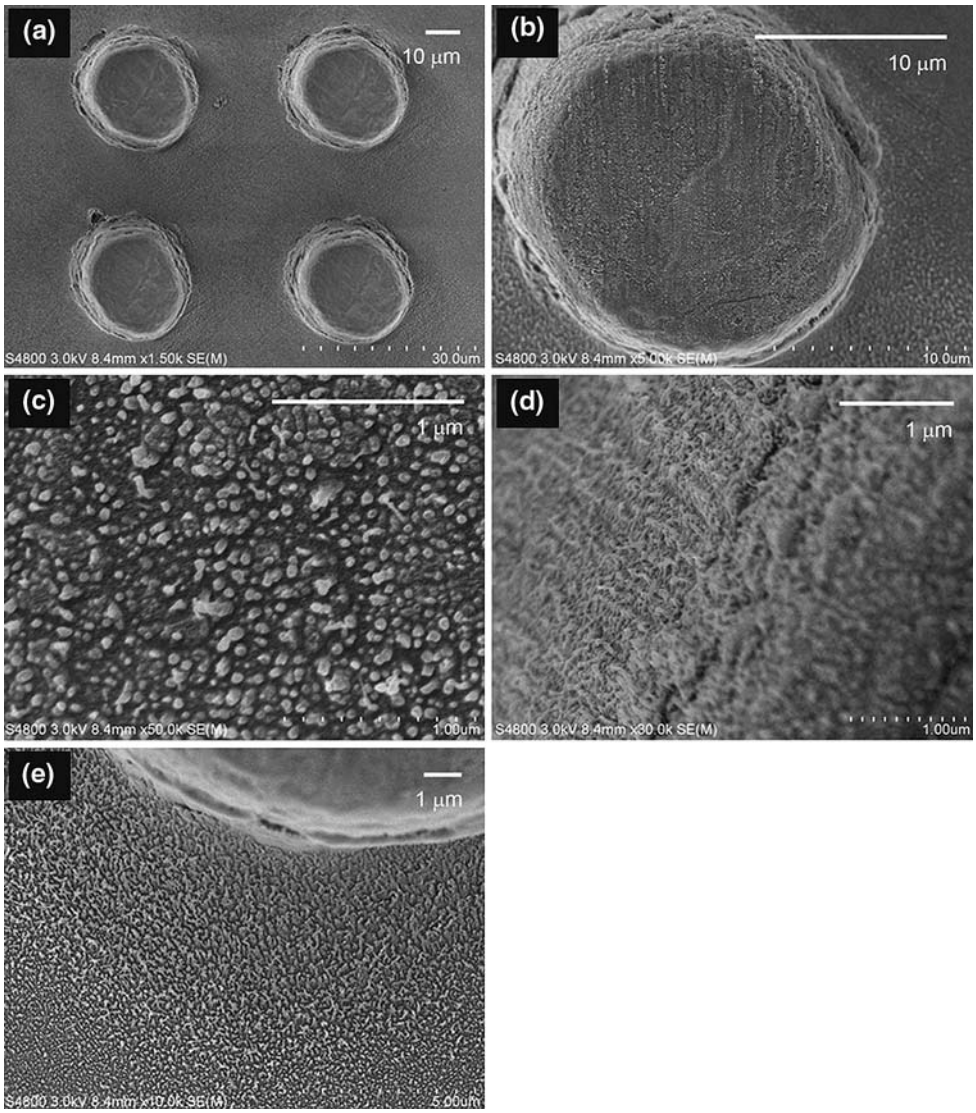

Fig. 1 SEM images of micro- and nano-structures. The view of a micro-pillar (**a**) shows nanostructuring on top of the pillar (**b**-**c**). The nanostructure covers the sides of the micropillars (**d**) as well as the plateau between the pillars (**e**)

After deposition, the samples were sonicated for a few minutes in 7X detergent (OneMed Ltd, Vantaa, Finland) and rinsed many times in de-ionized water. Then the samples were sonicated for a few minutes in ethanol and rinsed many times in sterile water before cells were added.

2.4 Atomic force microscope (AFM) characterization of the surface

Surface roughnesses were measured using a PSIA XE-100 (Park Systems Corp., Suwon, Korea) atomic force microscope which enables accurate imaging in nanoscale. Acta-10 (ST Instruments B.V., LE Groot-Ammers, The Netherlands) aluminium-coated silicon cantilevers were used in a non-contact mode. AFM characterization was realized for smooth PP samples and for smooth coated samples to clarify that the coating actually has not an influence on the surface roughness. The nanostructured area upon the micropillars was measured for uncoated and coated MNST samples to clarify whether the sputter cleaning and coating process can influence the nanostructures. Average surface roughness (R_a) and peak-to-valley roughness (R_{pv}) measurements were randomly taken at three different locations on six samples per group. The scan size was 2×2 μm^2. The scan rate was kept below 0.25 Hz while the Z voltage gain varied between 1 and 3. The roughness data were analyzed from the images using the instrument software.

2.5 Contact angle and surface energy measurements

Contact angles were obtained using the sessile drop (15 µl) method with a custom made apparatus based on an optical microscope SZ-PT Olympus equipped with a digital camera Olympus Camedia C-3030ZOOM (Olympus Corp., Tokyo, Japan). Before the measurements were made, the sample surfaces were treated by ultrasonic cleaning in ethanol for 2 min, then rinsed by ultrasonic cleaning in purified water for 2 min, and finally dried. The contact angles for two liquids, water and diiodomethane were measured within 5 s after placing the drop under constant conditions (22°C temperature and 45% relative humidity) on the surface. The spreading pressure was not taken into account. The drop image was stored in a digital camera, and image analysis software GIMP (www.gimp.org) was used to determine the contact angle from the shape geometry of the drop. For each liquid, five sessile drops for each sample were analyzed, for left and right sides, and finally the average contact angle was calculated.

The surface energies of the different samples were calculated using the Owens–Wendt theoretical model [46]. The dispersive γ_S^D and polar γ_S^P components of the samples surface energy were estimated using the geometrical equation,

$$(1+\cos\theta)\gamma_L = 2\left((\gamma_S^D\gamma_L^D)^{1/2} + (\gamma_S^P\gamma_L^P)^{1/2}\right) \quad (1)$$

where the superscript D labels the dispersive component and P the polar component of the surface tension and the subscripts S and L stand for solid and liquid, respectively. The dispersive component is related to van der Waals and other non-site specific interactions between the solid surface and the liquid used for the analysis. Hydrogen bonding, dipole–dipole, dipole-induced dipole and other site-specific interactions refers to the polar component. The known surface energy parameters of these liquids used in calculations are $\gamma_L = 72.8$ mJ/m^2, $\gamma_L^D = 21.8$ mJ/m^2 and $\gamma_L^P = 51.0$ mJ/m^2 for water and $\gamma_L = 50.8$ mJ/m^2, $\gamma_L^D = 50.8$ mJ/m^2 and $\gamma_L^P = 0.0$ mJ/m^2 for diiodomethane [47]. The total surface energy γ_S is the sum of its dispersive and polar components.

2.6 Cell culture

Human osteogenic sarcoma cells (Saos-2) were cultured in Dulbecco's Modified Eagle's medium (DMEM, Euroclone, Pero, Italy) containing 10% fetal calf serum (FCS, PAA, Linz, Austria), 2 mM L-glutamine (Sigma-Aldrich, St. Louis, MO, USA), 200 IU/ml of penicillin (Euroclone, Pero, Italy), 200 µg/ml of streptomycin (Euroclone), 2.5 µg/ml of fungizone (Sigma) and 50 µg/ml of ascorbic acid (Sigma). The cells were seeded on top of different samples (10×10 mm^2) by adding a medium, which contained 1.0×10^5 cells/ml to each sample cultured in separate cell culture plates (Greiner Bio-One, Frickenhausen, Germany). The cells were cultured for 48 h at 37°C in a 5% CO_2 atmosphere. Six samples of each material were used per experiment and testing was repeated twice.

2.7 SEM analysis of cultured cells

After cultivation for 48 h, the cells were fixed with 2.5% w/v glutaraldehyde (Sigma) in sodium cacodylate buffer (pH 7.4), and dehydrated with ethanol gradient and hexamethyldisilazane (Sigma). The specimens were covered with gold by sputtering (Sputter Coater E 5100, Polaron Equipment Ltd, England), and examined in a scanning electron microscope XL30 ESEM TMP (FEI Company/Oy Philips Ab, Brno, Czech Republic) at an accelerating voltage of 15–20 kV.

2.8 Cell number assay

The cellular contents attached to various surfaces were determined with the MTT colorimetric assay. At the end of the culture period of 48 h, the medium was changed to fresh medium, 0.5 mg/ml of MTT (Sigma) was added, and the medium was removed after incubation for 2 h. The

wells were washed with phosphate buffer, formazan salts were dissolved with 1000 µl of dimethylsulphoxide (DMSO)/ethanol (1:1), and the absorbance was measured at 595 nm with an ELISA reader. The number of cells was determined using a standard curve normalized to the number of osteoblast-like cells.

2.9 Statistical analysis

One-way ANOVA (SPSS 16.0 software) variance analysis followed by Tukey Post-Hoc Tests was applied to determine the statistical significance of the differences observed between groups. $P < 0.05$ was considered as significant. Data were expressed as mean ± standard deviation.

3 Results

3.1 Surface roughness and topographical characterization

The surface morphology of smooth and MNST PP samples was studied by AFM. The measured average surface roughness (R_a) and peak-to-valley roughness (R_{pv}) values indicated that the surfaces of injection molded PP were very planar and that the deposition of C_3N_4-Si film had not changed the surface morphology. At the top of the pillar, the uncoated MNST samples clearly displayed nanoscale rough characteristics (Fig. 2a) as already observed by SEM (Fig. 1c). However, in the C_3N_4-Si coated MNST samples, the nanostructuring at the top of the pillars was partly flattened (Fig. 2b and Table 1). This is probably due to the plasma cleaning procedure used prior to deposition to remove possible surface contamination and water as a way to guarantee good adhesion for the coating.

3.2 Contact angle and surface energy components

Table 2 gives the contact angles obtained by the sessile drop method on the different surfaces. The different components of surface energy are illustrated in Fig. 3. With uncoated samples and with both liquids (water and diiodomethane) the contact angles increased in order to smooth, MST and MNST. The contact angles of coated samples were notably lower than their uncoated counterparts (Table 2 and Fig. 4).

Table 1 Surface roughness values, average surface roughness (R_a) and peak-to-valley roughness (R_{pv}), of tested materials determined using AFM

Material	R_{pv} (nm)	R_a (nm)
Smooth, uncoated[#]	21 ± 4	4 ± 1
Smooth, coated[#]	19 ± 4	4 ± 1
MNST[a], uncoated*	66 ± 27	16 ± 7
MNST[a], coated	30 ± 17	7 ± 5

[a] *MNST* micro-and nano-structured

* denotes significant difference ($P < 0.01$) compared to all sample groups

[#] denotes significant difference ($P < 0.01$) compared to micro- and nano-structured, uncoated sample group

3.3 Scanning electron microscopical observations

The cells on smooth uncoated PP surface became attached mainly as single cells, and they remained rounded in shape, suggesting that only a minimal number of focal adhesions

Table 2 Contact angles of tested samples determined by sessile drop method

Sample	Contact angle, θ (°)			
	Uncoated		Coated	
	θ^w	θ^d	θ^w	θ^d
Smooth	97.1 ± 1.7	54.7 ± 1.1	63.0 ± 1.5	39.6 ± 2.4
MST[a]	136.1 ± 1.9	64.3 ± 1.3	69.1 ± 0.9	44.3 ± 1.5
MNST[b]	146.2 ± 1.6	72.5 ± 1.6	53.5 ± 1.4	30.6 ± 1.4

There is a significant difference ($P < 0.01$) in contact angles between all materials

[a] *MST* microstructured

[b] *MNST* micro-and nano-structured

[d] diiodomethane

[w] water

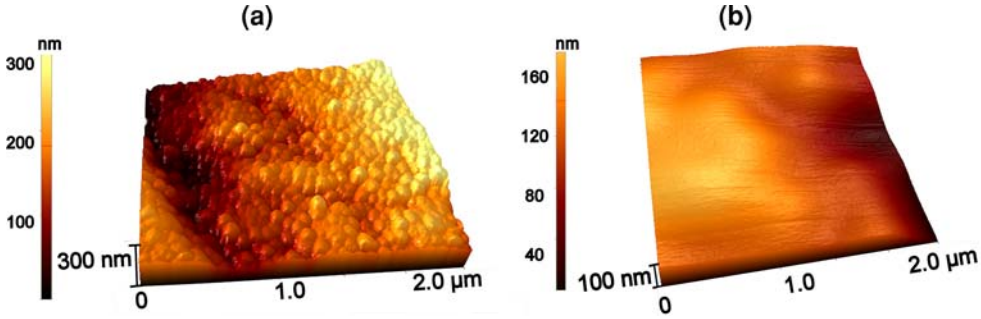

Fig. 2 AFM images of surfaces of micro- and nano-structured (MNST) samples on top of the micro-pillar. Nanostructures are clearly visible in the uncoated MNST sample (**a**), whereas the surface is partly flattened in the coated MNST material (**b**)

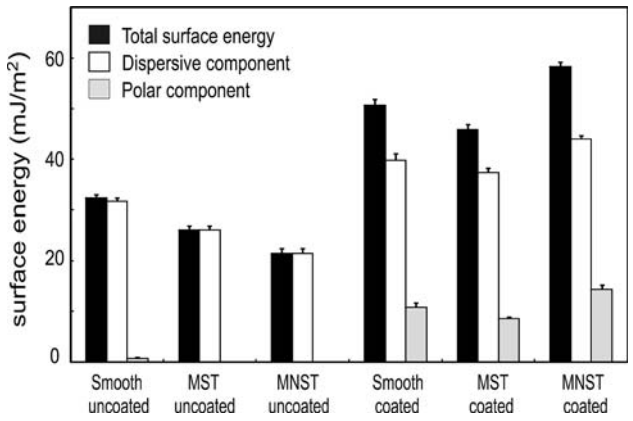

Fig. 3 Total surface free energy (γ_S) and its' dispersive (γ_S^D) and polar (γ_S^P) components for smooth, microstructured (MST) and micro- and nano-structured (MNST) samples with and without C_3N_4-Si coating calculated using the Owens–Wendt approach [46]. Error bars indicate standard deviations

had been formed (Fig. 5a, e, i). Coating of smooth surface with C_3N_4–Si clearly enhanced the attachment properties of cells. The cells appeared to be mainly in contact with each other and their morphology had switched to being flattened and spread out (Fig. 5b, f, j). In the same way as the smooth, uncoated PP, the uncoated MNST was not an

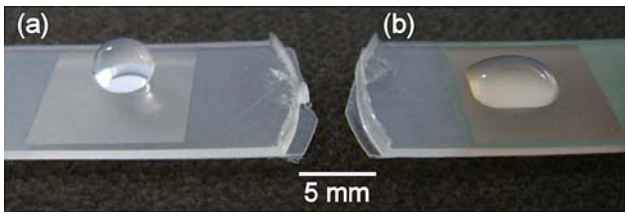

Fig. 4 A water droplet on the **a** uncoated and **b** Coldab^{TM} (Picodeon Ltd) coated micro- and nano-structured PP surfaces. Note the difference in droplet shapes. Only the rectangular patterned areas were used for cell studies

ideal surface for osteoblast-like cells attachment. However, one major difference was that the osteoblast-like cells tended to grow in cell clusters with an apparent three-dimensional structure (Fig. 5c, g, k). The coating of MNST also promoted a higher number of cells attached on the surface 48 h after cell seeding (Fig. 5d, h, l). The differences in the coated MNST and MST surfaces can be seen in Fig. 6. The cells mainly used the plateau between the micropillars for attachment on the MST surfaces (Fig. 6b), in contrast to the situation with the MNST surfaces where osteoblast-like cells were attached on top of the pillars and formed cellular extensions to the edges of the neighbouring nanostructured pillars (Fig. 6a).

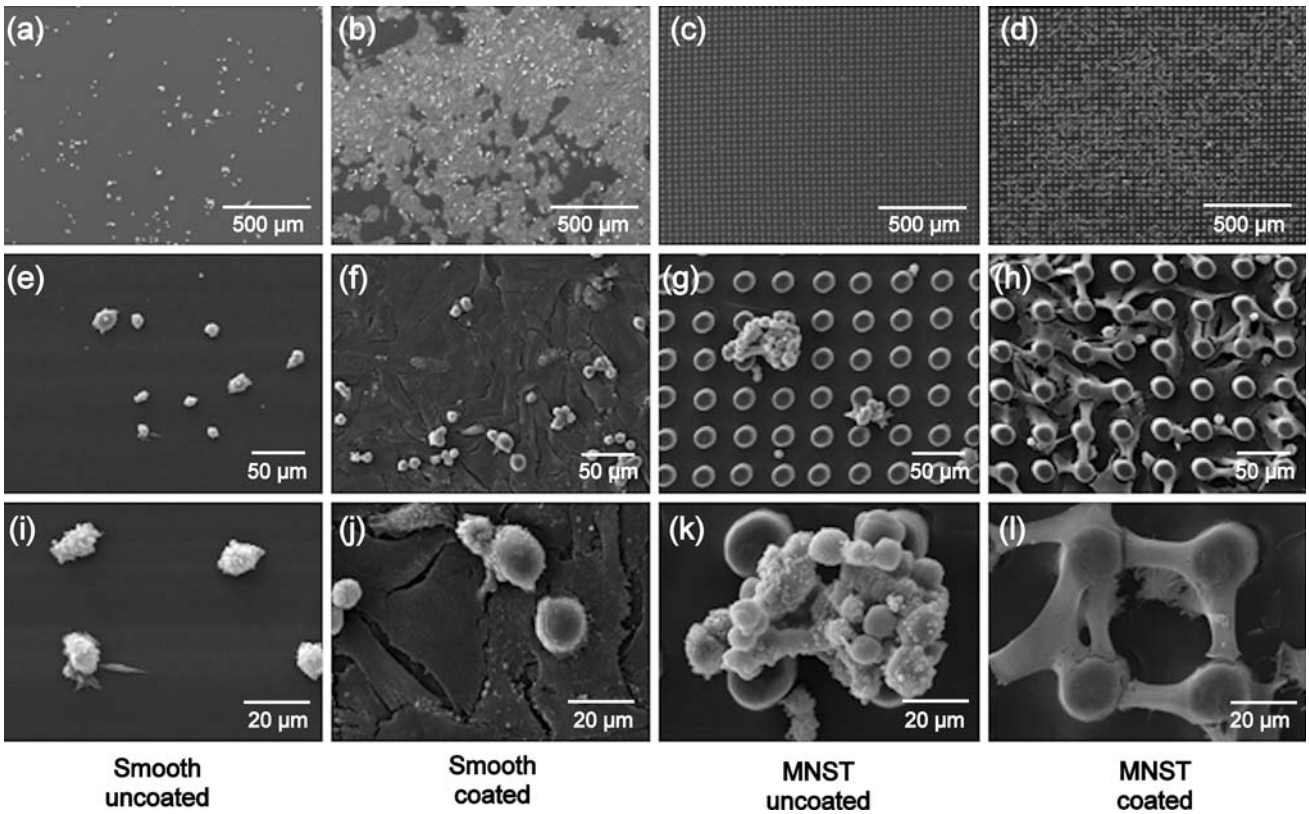

Fig. 5 SEM images of Saos-2 cells after 48 h culture period grown on smooth uncoated (**a**, **e**, **i**), smooth coated (**b**, **f**, **j**), micro- and nano-structured (MNST) uncoated (**c**, **g**, **k**), and MNST coated (**d**, **h**, **l**) samples at three different magnifications

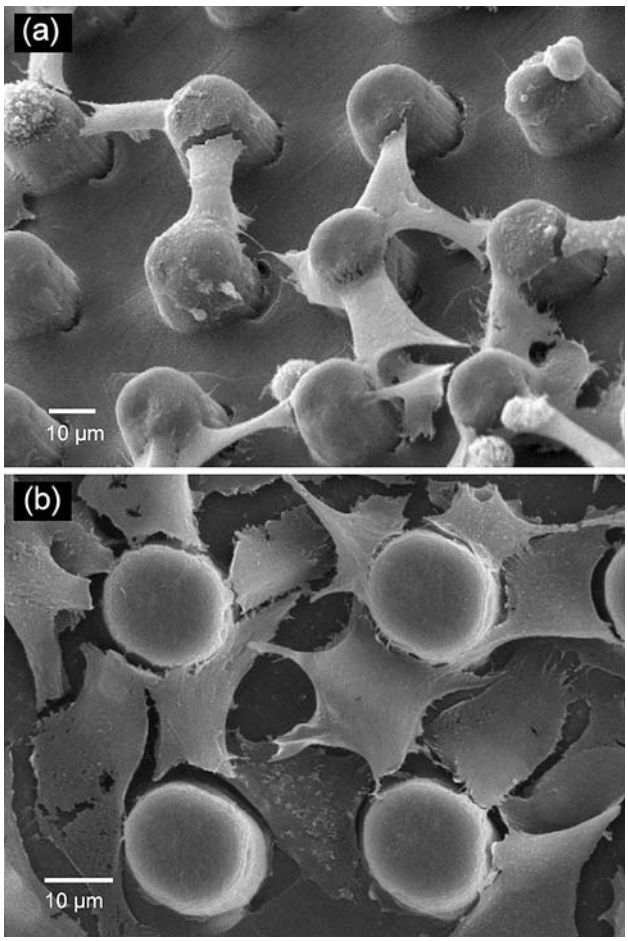

Fig. 6 SEM images of Saos-2 cells after 48 h culture period grown on micro- and nano-structured (MNST) coated (**a**) and microstructured (MST) coated sample (**b**)

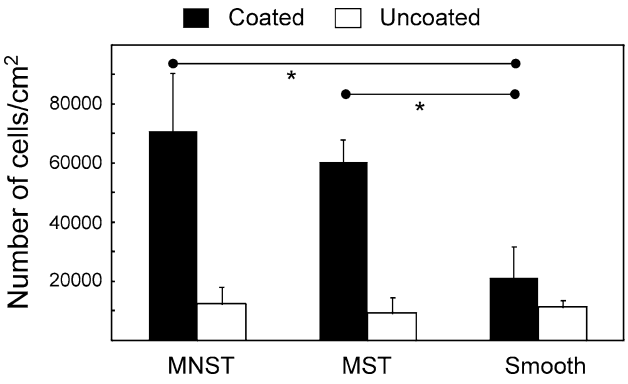

Fig. 7 The number of Saos-2 cells at 48 h from seeding on coated and uncoated micro- and nano-structured (MNST), microstructured (MST) and smooth surfaces. The presence of viable cells was spectrophotometrically assessed by the MTT assay and a standard curve normalized to the number of osteoblast-like cells. * denotes significant difference $P < 0.01$. Error bars indicate standard deviation

3.4 Cell number analysis

The MTT assay used in this study relates to the number cells attached on the surfaces 48 h after the cell seeding (Fig. 7). Since the properties of the examined surfaces differ greatly, the factors determining the final cell number at the end of experiment clearly involved the extent of original cell attachment and their proliferation rate. It was noticed that the number of attached cells on C_3N_4-Si coated MST and MNST samples was significantly greater than on the uncoated samples ($P < 0.01$). The highest cell number was observed on C_3N_4-Si coated MNST sample, though it was not statistically different from that on the C_3N_4-Si coated MST sample. No significant differences among the uncoated smooth and structured samples were observed.

4 Discussion

In the present study, we examined the effects of the combination of surface texturing and thin film deposition on the adhesion, spreading and contact guidance of Saos-2 cells. C_3N_4-Si coated MST and MNST surfaces proved to possess very favourable combinations of these surface properties in comparison to the uncoated or unstructured ones in terms of biological performance, i.e., cell adhesion, the number of cells attached (even 500% increase) and contact guidance. The results of this study revealed that the higher surface energy was a very important variable, but not alone sufficient to promote a marked increase in osteoblast-like cells responses to substrates without surface texturing.

Surface topography and surface free energy are two important factors that regulate cell responses to biomaterials. Increased wettability with higher surface energy has been shown to enhance interaction between an implant surface and osteoblasts [23, 24]. When implants with increased hydrophilicity are implanted in bone, the rate and extent of bone formation are increased, supporting the hypothesis that surface energy does promote bone cell maturation and differentiation [48]. In our study, we used highly hydrophobic PP substrates which were structured in micro- and nano-scale. In hydrophobic materials, patterning increases the hydrophobic nature of material. PP was chosen as a model material due to its favourable processing characteristics to be modified by the injection molding technique, a process that can be used to fabricate topographically patterned substrates with rounded micro- and nano-structures for many thermoplastic polymer biomaterials. Half of the substrates were coated with biocompatible C_3N_4-Si thin films to make the surface properties more hydrophilic. In principle, if the coating would completely seal the substrate surface, then the sample properties would predominantly reflect those of the coating material. The

USPLD technique enables the manufacture of coatings, which are equally smooth, an important parameter when considering the wettability properties of surfaces in terms of cell adhesion and spreading. In this study, we managed to reduce the contact angles of PP surfaces drastically. Before deposition of C_3N_4-Si coating, the substrates were gently cleaned with an ion beam. This cleaning process partly destroyed the nanoscale structuring (Fig. 2b) and thus the effect on osteoblast-like cells behavior is not as clear as the case might be. However, the nanostructuring still existed in a large area of the samples. This is reflected in the contact angle values which were smallest for the coated MNST samples (Table 2) and from the different behavior of osteoblast-like cells in coated MNST and MST samples (Fig. 6). The contact angles of coated MST samples were larger than the contact angles of the coated smooth samples. This is due to the fact that even fairly thin coating deposited using the Coldab^{TM} method was unable to fully cover the surface of micro-pillars with high aspect ratios. In the future, it may be possible to optimize these features by changing texturing features, the ion beam cleaning procedure or some aspects of the coating process.

CN_x films have shown promising properties when tested with osteoblasts [28, 49, 50], endothelial cells [30, 51], macrophages and fibroblasts [52], and furthermore these films have proven hemocompatiblity [30, 33]. However, considerable attention has recently been focused on the biocompatibility of DLC and its hybrids, but it is difficult to find any reports on the biocompatibility of CN_x coatings with dopants, especially of the stoichiometric C_3N_4 studied here. It is known that CN_x has similar structural characteristics to DLC and its favourable mechanical and tribological properties are comparable to that of DLC. In addition, it is likely that the presence of nitrogen has a positive effect on biocompatibility [53, 54]. Okpalugo et al. demonstrated that the number of attached endothelial cells was highest on Si-DLC, followed by the N-DLC and undoped DLC. They also reported that in addition to the wettability, the semiconductive properties and the reduced stress of the films can evoke interactions with human microvascular endothelial cells [53]. The enhanced adhesion and spreading of osteoblast-like cells on C_3N_4-Si coated surfaces is not just simply related to improved wettability but may also be related to changes in the material's micro and atomic structural properties induced by the presence of atomic nitrogen and silicon, e.g., changes in the electronic properties. Detailed features of C_3N_4-Si and other carbon nitride composites related to cell adhesion and profileration will be studied in forthcoming articles.

There are a large number of papers which have examined the micro-and nano-sized patterning effects on cell alignment [9, 55], morphology [6, 56], proliferation [57–59] as well as gene expression and differentiation [60, 61] but nonetheless we have limited understanding of the mechanisms accounting for the substrate topography and the mechanical cell signaling that it creates. Flemming et al. and Martinez et al. have summarized the substrate topographical effects on cell behavior. These studies mainly concentrated on to the microgrooves, and revealed that cells aligned along the long axis of the grooves, while actin and other cytoskeletal elements were organized in an orientation parallel to the grooves [6, 62]. Interactions between cells and other features, such as pillars and wells, have been more rarely studied. Rea et al. demonstrated that cell alignment was also seen along pillars and wells when culturing MG-63 and Saos-2 cells on bioactive composites filled with high-density polyethylene substrates [57]. They also noted like Green et al. that pillar formations increased cell proliferation and density in comparison to surfaces patterned with wells [57, 58]. Mata et al. reported that posts which were 10 μm-in-diameter exhibited a greater cell number than did smooth or 5, 20, and 40 μm-in-diameter posts when human connective tissue progenitor cells were cultured on PDMS surfaces [63]. On the other hand, textures in the size range of 0.5–2 μm-in-diameter were reported to be most effective in promoting UMR osteoblast-like cell adhesion to chlorotrifluoroethylene (Aclar) substrates precoated with highly purified bovine serum albumin [64]. Pillar arrays have also been claimed to influence astroglial cell attachment, growth and morphology [65]. A continuous edge of surface feature was not a prerequisite for guided cell migration in fibroblasts and epithelial cells [66] as well as osteoblastic cells [67]. Microscale pillars have also shown to influence both cell alignment and the cellular microenvironment and thus be of potential importance in the field of bone regeneration [67]. In the present study, we fabricated 20 μm-in-diameter and 20 μm-high with rounded tops. On the smooth PP surfaces, the osteoblast-like cells grew mostly as single rounded cells, while on C_3N_4-Si coated material, the cells adopted a broad flattened shape and adhered well to the surface. The flat shape of the cells on the coated surfaces suggests that these cells had formed more numerous focal adhesions than the cells grown on uncoated materials. Cells on the structured C_3N_4-Si coated surfaces tended to became attached next to the pillars and spread between them while directing their processes from pillar to pillar towards other cells. The morphology of Saos-2 cells was also more elongated than on C_3N_4-Si coated smooth surfaces, with the cells displaying classical aspects of polygonal spreading. Interestingly, on the coated MNST surface, the osteoblast-like cells preferred to attach to the top of the pillars and formed cellular extensions to the edges of the neighbouring nanostructured pillars (Fig. 6a). In contrast, on the coated MST surfaces, cells mainly used the bottom area between the micropillars for attachment due to the

lack of a nanostructured adhering surface (Fig. 6b). On uncoated MNST surfaces, the cells adopted a cluster-type 3-dimensional growth pattern (Fig. 5c, g, k). This property could be useful for expansion of some other types of cells, such as chondrocytes, as soon as a compromise between the morphology and cell growth can be found. Furthermore, both microtexturing and micro-and nano-texturing in C_3N_4-Si coated surfaces led to about 200% increase in cell number/area compared to the C_3N_4-Si coated smooth surfaces. Overall the surfaces structured with micro-pillars with nanotexturing all over the area were best for cellular accumulation. Puckett et al. demonstrated that narrowing the width of the nano-rough regions (from 80 μm to 22 μm) on the patterned Ti surfaces resulted in a decreased number of osteoblasts adhering to these areas, and also evoked changes in the osteoblast morphology [56]. Since the size of an osteoblast is around 20–30 μm-in-diameter, too small regions makes it difficult for these cells to became attached and extend cellular processes. With the injection molding technique, the area of micro- and nano-structuring can be easily modified. One other advantage of this technique is also the rounded shape in the top of the feature. Since it is well-known that features with sharp edges are not common in the body and also rounded features have reported to influence cell alignment [68].

In our study, there were 86% more cells in the smooth C_3N_4-Si coated PP compared to smooth uncoated PP and 551%/476% more cells with MST/MNST C_3N_4-Si coated PP than could be obtained with MST/MNST uncoated PP. This result is accordance with the reports of Khang et al. and Feng et al. i.e., the greater surface roughness and higher surface energy resulted in greater numbers of adhering osteoblasts on Ti surfaces [24, 69]. Also Zhao et al. demonstrated that the combination of high surface energy and topography had a synergistic effect to promote osteocalcin production in the cells on the Ti surfaces [70]. We also detected a synergistic effect of high surface energy and microtexturing or micro- and nano-texturing which enhanced the interactions between the osteoblast-like cells and potential implant material.

5 Conclusion

The combination of injection molding and ultra-short pulsed laser deposition techniques has proven to be a useful tool for fabricating micro- and nano-structured surfaces with which to study cell–substrate interactions. This study also examined the effect of surface energy and surface texturing on osteoblast-like cells adhesion and spreading with smooth, MST and MNST PP surfaces. The hydrophilic nature of PP samples was achieved by applying a biocompatible C_3N_4-Si coating. Overall, the results of the presented study showed that micro- and nano-texturing combined with high surface energy achieved by a proper coating significantly improved the adhesion, spreading, and contact guidance of osteoblast-like cells in vitro.

Acknowledgments This study was supported by the PhD-programme in Musculoskeletal Diseases and Biomaterials, Joint Research Program in Materials Science of Kuopio and Joensuu Universities and the Otto A. Malm Foundation. The authors thank Picodeon Ltd Oy, Helsinki, Finland for providing Coldab™ thin film depositions. Ari Halvari and Mikko Laasanen from Microsensor Laboratory are thanked for AFM imaging. Laboratory assistant Sanna Miettinen, technical assistant Juhani Hakala and the staff of BioMater Centre from the University of Kuopio are acknowledged for their technical support. We also thank Ewen MacDonald for language editing.

References

1. Curtis A, Wilkinson C. Topographical control of cells. Biomaterials. 1997;18:1573–83. doi:10.1016/S0142-9612(97)00144-0.
2. Puleo DA, Nanci A. Understanding and controlling the bone-implant interface. Biomaterials. 1999;20:2311–21. doi:10.1016/S0142-9612(99)00160-X.
3. Schwartz Z, Boyan BD. Underlying mechanisms at the bone-biomaterial interface. J Cell Biochem. 1994;56:340–7. doi:10.1002/jcb.240560310.
4. Harrison RG. The cultivation of tissues in extraneous media as a method of morpho-genetic study. Anat Rec. 1912;6:181–93. doi:10.1002/ar.1090060404.
5. Charest JL, Bryant LE, Garcia AJ, King WP. Hot embossing for micropatterned cell substrates. Biomaterials. 2004;25:4767–75. doi:10.1016/j.biomaterials.2003.12.011.
6. Flemming RG, Murphy CJ, Abrams GA, Goodman SL, Nealey PF. Effects of synthetic micro- and nano-structured surfaces on cell behavior. Biomaterials. 1999;20:573–88. doi:10.1016/S0142-9612(98)00209-9.
7. Mwenifumbo S, Li M, Chen J, Beye A, Soboyejo W. Cell/surface interactions on laser micro-textured titanium-coated silicon surfaces. J Mater Sci Mater Med. 2007;18:9–23. doi:10.1007/s10856-006-0658-9.
8. Ismail FS, Rohanizadeh R, Atwa S, Mason RS, Ruys AJ, Martin PJ, et al. The influence of surface chemistry and topography on the contact guidance of MG63 osteoblast cells. J Mater Sci Mater Med. 2007;18:705–14. doi:10.1007/s10856-006-0012-2.
9. den Braber ET, de Ruijter JE, Smits HTJ, Ginsel LA, von Recum AF, Jansen JA. Quantitative analysis of cell proliferation and orientation on substrata with uniform parallel surface micro-grooves. Biomaterials. 1996;17:1093–9. doi:10.1016/0142-9612(96)85910-2.
10. Levy S, Van Dalen M, Agonafer S, Soboyejo WO. Cell/surface interactions and adhesion on bioactive glass. J Mater Sci Mater Med. 2007;18:89–102. doi:10.1007/s10856-006-0666-9.
11. Gough JE, Notingher I, Hench LL. Osteoblast attachment and mineralized nodule formation on rough and smooth 45S5 bioactive glass monoliths. J Biomed Mater Res A. 2004;68:640–50. doi:10.1002/jbm.a.20075.
12. Schmidt JA, von Recum AF. Macrophage response to micro-textured silicone. Biomaterials. 1992;13:1059–69. doi:10.1016/0142-9612(92)90138-E.
13. Wang JH-C, Grood ES, Florer J, Wenstrup R. Alignment and proliferation of MC3T3-E1 osteoblasts in microgrooved silicone

substrata subjected to cyclic stretching. J Biomech. 2000;33:729–35. doi:10.1016/S0021-9290(00)00013-0.
14. van Kooten TG, von Recum AF. Cell adhesion to textured silicone surfaces: the influence of time of adhesion and texture on focal contact and fibronectin fibril formation. Tissue Eng. 1999;5:223–40. doi:10.1089/ten.1999.5.223.
15. Madou MJ. Fundamentals of microfabrication: the science of miniaturization. 2nd ed. CRC Press: Boca Raton, FL; 2002. p. 1–76.
16. Xia Y, Whitesides GM. Soft lithography. Annu Rev Mater Sci. 1998;28:153–84. doi:10.1146/annurev.matsci.28.1.153.
17. Puukilainen E, Rasilainen T, Suvanto M, Pakkanen TA. Superhydrophobic polyolefin surfaces: controlled micro- and nanostructures. Langmuir. 2007;23:7263–8. doi:10.1021/la063588h.
18. Puukilainen E, Koponen HK, Xiao Z, Suvanto S, Pakkanen TA. Nanostructured and chemically modified hydrophobic polyolefin surfaces. Colloids Surf A Physicochem Eng Asp. 2006;287:175–81. doi:10.1016/j.colsurfa.2006.03.056.
19. Koponen HK, Saarikoski I, Korhonen T, Pääkkö M, Kuisma R, Pakkanen TT, et al. Modification of cycloolefin copolymer and poly(vinyl chloride) surfaces by superimposition of nano- and microstructures. Appl Surf Sci. 2007;253:5208–13. doi:10.1016/j.apsusc.2006.11.039.
20. Miikkulainen V, Rasilainen T, Puukilainen E, Suvanto M, Pakkanen TA. Atomic layer deposition as pore diameter adjustment tool for nanoporous aluminum oxide injection molding masks. Langmuir. 2008;24:4473–7. doi:10.1021/la800285s.
21. Hallab NJ, Bundy KJ, O'Connor K, Moses RL, Jacobs JJ. Evaluation of metallic and polymeric biomaterial surface energy and surface roughness characteristics for directed cell adhesion. Tissue Eng. 2001;7:55–71. doi:10.1089/107632700300003297.
22. van Kooten TG, Schakenraad JM, van der Mei HC, Busscher HJ. Influence of substratum wettability on the strength of adhesion of human fibroblasts. Biomaterials. 1992;13:897–904. doi:10.1016/0142-9612(92)90112-2.
23. Lim JY, Shaughnessy MC, Zhou Z, Noh H, Vogler EA, Donahue HJ. Surface energy effects on osteoblast spatial growth and mineralization. Biomaterials. 2008;29:1776–84. doi:10.1016/j.biomaterials.2007.12.026.
24. Khang D, Lu J, Yao C, Haberstroh KM, Webster TJ. The role of nanometer and sub-micron surface features on vascular and bone cell adhesion on titanium. Biomaterials. 2008;29:970–83. doi:10.1016/j.biomaterials.2007.11.009.
25. Zhao G, Schwartz Z, Wieland M, Rupp F, Geis-Gerstorfer J, Cochran DL, et al. High surface energy enhances cell response to titanium substrate microstructure. J Biomed Mater Res A. 2005;74:49–58. doi:10.1002/jbm.a.30320.
26. Amberla T, Rekow M, Köngäs J, Asonen H, Salminen T, Viitanen N, Kulmala M, Vuoristo P, Pessa M, Lappalainen R. In: Proceedings of the 49th annual technical conference. Washington, DC; 2006. p. 79.
27. Liu AY, Cohen ML. Prediction of new low compressibility solids. Science. 1989;245:841–2. doi:10.1126/science.245.4920.841.
28. Du C, Su XW, Cui FZ, Zhu XD. Morphological behaviour of osteoblasts on diamond-like carbon coating and amorphous C-N film in organ culture. Biomaterials. 1998;19:651–8. doi:10.1016/S0142-9612(97)00159-2.
29. Cui FZ, Li DJ. A review of investigations on biocompatibility of diamond-like carbon and carbon nitride films. Surf Coat Tech. 2000;131:481–7. doi:10.1016/S0257-8972(00)00809-4.
30. Cui FZ, Qing XL, Li DJ, Zhao J. Biomedical investigations on CN_x coating. Surf Coat Tech. 2005;200:1009–13. doi:10.1016/j.surfcoat.2005.02.157.
31. Rodil SE, Olivares R, Arzate H. In vitro cytotoxicity of amorphous carbon films. Biomed Mater Eng. 2005;15:101–12.
32. Rodil SE, Olivares R, Arzate H, Muhl S. Properties of carbon films and their biocompatibility using in-vitro tests. Diam Relat Mater. 2003;12:931–7. doi:10.1016/S0925-9635(02)00217-0.
33. Kwok SCH, Yang P, Wang J, Liu X, Chu PK. Hemocompatibility of nitrogen-doped, hydrogen-free diamond-like carbon prepared by nitrogen plasma immersion ion implantation-deposition. J Biomed Mater Res A. 2004;70:107–14. doi:10.1002/jbm.a.30070.
34. Boyd KJ, Marton D, Todorov SS, Al-Bayati AH, Kulik J, Zuhr RA, et al. Formation of C–N thin films by ion beam deposition. J Vac Sci Technol A. 1995;13:2110–22. doi:10.1116/1.579528.
35. Lopez S, Dunlop HM, Benmalek M, Tourillon G, Wong M-S, Sproul WD. XPS, XANES and ToF-SIMS characterization of reactively magnetron-sputtered carbon nitride films. Surf Interface Anal. 1997;25:315–23. doi:10.1002/(SICI)1096-9918(199705)25:5<315::AID-SIA238>3.0.CO;2-S.
36. Baker MA, Hammer P. Study of the chemical composition and microstructure of ion beam-deposited CN_x films including an XPS C 1s peak simulation. Surf Interface Anal. 1997;25:301–14. doi:10.1002/(SICI)1096-9918(199705)25:5<301::AID-SIA236>3.0.CO;2-A.
37. Dawei W, Dejun F, Huaixi G, Zhihong Z, Xianquan M, Xiangjun F. Structure and characteristics of C_3N_4 thin films prepared by rf plasma-enhanced chemical vapor deposition. Phys Rev B. 1997;56:4949–54. doi:10.1103/PhysRevB.56.4949.
38. Gouzman I, Brener R, Hoffman A. Nitridation of diamond and graphite surfaces by low energy N+2 ion irradiation. Surf Sci. 1995;331–333:283–8. doi:10.1016/0039-6028(95)00187-5.
39. Franco LM, Pérez JA, Riascos H. Chemical analysis of CN_x thin films produced by pulsed laser ablation. Microelectron J. 2008;39:1363–5. doi:10.1016/j.mejo.2008.01.091.
40. Zhao Q, Liu Y, Wang C, Wang S. Bacterial adhesion on silicon-doped diamond-like carbon films. Diam Relat Mater. 2007;16:1682–7. doi:10.1016/j.diamond.2007.03.002.
41. Wan GJ, Yang P, Fu RKY, Mei YF, Qiu T, Kwok SCH, et al. Characteristics and surface energy of silicon-doped diamond-like carbon films fabricated by plasma immersion ion implantation and deposition. Diam Relat Mater. 2006;15:1276–81. doi:10.1016/j.diamond.2005.09.042.
42. Borisenko KB, Evangelou EA, Zhao Q, Abel EW. Contact angles of diiodomethane on silicon-doped diamond-like carbon coatings in electrolyte solutions. J Colloid Interface Sci. 2008;326:329–32. doi:10.1016/j.jcis.2008.06.045.
43. Bendavid A, Martin PJ, Comte C, Preston EW, Haq AJ, Magdon Ismail FS, et al. The mechanical and biocompatibility properties of DLC-Si films prepared by pulsed DC plasma activated chemical vapor deposition. Diam Relat Mater. 2007;16:1616–22. doi:10.1016/j.diamond.2007.02.006.
44. Roy RK, Choi HW, Yi JW, Moon M-W, Lee K-R, Han DK, et al. Hemocompatibility of surface-modified, silicon-incorporated, diamond-like carbon films. Acta Biomater. 2009;5:249–56. doi:10.1016/j.actbio.2008.07.031.
45. Liu C, Zhao Q, Liu Y, Wang S, Abel EW. Reduction of bacterial adhesion on modified DLC coatings. Colloids Surf B Biointerfaces. 2008;61:182–7. doi:10.1016/j.colsurfb.2007.08.008.
46. Owens DK, Wendt RC. Estimation of the surface free energy of polymers. J Appl Polym Sci. 1969;13:1741–7. doi:10.1002/app.1969.070130815.
47. Oliveira AL, Malafaya PB, Reis RL. Sodium silicate gel as a precursor for the in vitro nucleation and growth of a bone-like apatite coating in compact and porous polymeric structures. Biomaterials. 2003;24:2575–84. doi:10.1016/S0142-9612(03)00060-7.
48. Eriksson C, Nygren H, Ohlson K. Implantation of hydrophilic and hydrophobic titanium discs in rat tibia: cellular reactions on the surfaces during the first 3 weeks in bone. Biomaterials. 2004;25:4759–66. doi:10.1016/j.biomaterials.2003.12.006.

49. Tessier PY, Pichon L, Villechaise P, Linez P, Angleraud B, Mubumbila N, et al. Carbon nitride thin films as protective coatings for biomaterials: synthesis, mechanical and biocompatibility characterizations. Diam Relat Mater. 2003;12:1066–9. doi:10.1016/S0925-9635(02)00314-X.
50. Olivares R, Rodil SE, Arzate H. In vitro studies of the biomineralization in amorphous carbon films. Surf Coat Tech. 2004; 177–178:758–64. doi:10.1016/j.surfcoat.2003.08.018.
51. Li D, Niu L. Influence of N atomic percentages on cell attachment for CN_x coatings. Bull Mater Sci. 2003;26:371–5. doi:10.1007/BF02711178.
52. Li DJ, Zhang SJ, Niu LF. Influence of NHn+ beam bombarding energy on structural characterization and cell attachment of CN_x coating. Appl Surf Sci. 2001;180:270–9. doi:10.1016/S0169-4332(01)00356-7.
53. Okpalugo TIT, Murphy H, Ogwu AA, Abbas G, Ray SC, Maguire PD, et al. Human microvascular endothelial cellular interaction with atomic N-doped DLC compared with Si-doped DLC thin films. J Biomed Mater Res B Appl Biomater. 2006;78:222–9. doi:10.1002/jbm.b.30459.
54. Okpalugo TIT, Ogwu AA, Okpalugo AC, McCullough RW, Ahmed W. The human micro-vascular endothelial cells in vitro interaction with atomic-nitrogen-doped diamond-like carbon thin films. J Biomed Mater Res B Appl Biomater. 2008;85:188–95. doi:10.1002/jbm.b.30934.
55. Clark P, Connolly P, Curtis ASG, Dow JAT, Wilkinson CDW. Topographical control of cell behaviour. Development. 1987; 99:439–48.
56. Puckett S, Pareta R, Webster TJ. Nano rough micron patterned titanium for directing osteoblast morphology and adhesion. Int J Nanomedicine. 2008;3:229–41.
57. Rea SM, Brooks RA, Schneider A, Best SM, Bonfield W. Osteoblast-like cell response to bioactive composites-surface-topography and composition effects. J Biomed Mater Res B Appl Biomater. 2004;70:250–61. doi:10.1002/jbm.b.30039.
58. Green AM, Jansen JA, van der Waerden JPCM, von Recum AF. Fibroblast response to microtextured silicone surfaces: texture orientation into or out of the surface. J Biomed Mater Res. 1994;28:647–53. doi:10.1002/jbm.820280515.
59. Keselowsky BG, Wang L, Schwartz Z, Garcia AJ, Boyan BD. Integrin alpha(5) controls osteoblastic proliferation and differentiation responses to titanium substrates presenting different roughness characteristics in a roughness independent manner. J Biomed Mater Res A. 2007;80:700–10. doi:10.1002/jbm.a.30898.
60. Jin CY, Zhu BS, Wang XF, Lu QH, Chen WT, Zhou XJ. Nanoscale surface topography enhances cell adhesion and gene expression of madine darby canine kidney cells. J Mater Sci Mater Med. 2008;19:2215–22. doi:10.1007/s10856-007-3323-z.
61. Bruinink A, Wintermantel E. Grooves affect primary bone marrow but not osteoblastic MC3T3-E1 cell cultures. Biomaterials. 2001;22:2465–73. doi:10.1016/S0142-9612(00)00434-8.
62. Martínez E, Engel E, Planell JA, Samitier J. Effects of artificial micro- and nano-structured surfaces on cell behaviour. Ann Anat. 2009;191:126–35. doi:10.1016/j.aanat.2008.05.006.
63. Mata A, Boehm C, Fleischman AJ, Muschler G, Roy S. Growth of connective tissue progenitor cells on microtextured polydimethylsiloxane surfaces. J Biomed Mater Res. 2002;62:499–506. doi:10.1002/jbm.10353.
64. Mata A, Su X, Fleischman AJ, Roy S, Banks BA, Miller SK, et al. Osteoblast attachment to a textured surface in the absence of exogenous adhesion proteins. IEEE Trans Nanobioscience. 2003;2:287–94. doi:10.1109/TNB.2003.820268.
65. Turner AMP, Dowell N, Turner SWP, Kam L, Isaacson M, Turner JN, et al. Attachment of astroglial cells to microfabricated pillar arrays of different geometries. J Biomed Mater Res. 2000;51:430–41. doi:10.1002/1097-4636(20000905)51:3<430::AID-JBM18>3.0.CO;2-C.
66. Hamilton DW, Brunette DM. "Gap guidance" of fibroblasts and epithelial cells by discontinuous edged surfaces. Exp Cell Res. 2005;309:429–37. doi:10.1016/j.yexcr.2005.06.015.
67. Hamilton DW, Wong KS, Brunette DM. Microfabricated discontinuous-edge surface topographies influence osteoblast adhesion, migration, cytoskeletal organization, and proliferation and enhance matrix and mineral deposition in vitro. Calcif Tissue Int. 2006;78:314–25. doi:10.1007/s00223-005-0238-x.
68. Bettinger CJ, Orrick B, Misra A, Langer R, Borenstein JT. Microfabrication of poly (glycerol–sebacate) for contact guidance applications. Biomaterials. 2006;27:2558–65. doi:10.1016/j.biomaterials.2005.11.029.
69. Feng B, Weng J, Yang BC, Qu SX, Zhang XD. Characterization of surface oxide films on titanium and adhesion of osteoblast. Biomaterials. 2003;24:4663–70. doi:10.1016/S0142-9612(03)00366-1.
70. Zhao G, Raines AL, Wieland M, Schwartz Z, Boyan BD. Requirement for both micron- and submicron scale structure for synergistic responses of osteoblasts to substrate surface energy and topography. Biomaterials. 2007;28:2821–9. doi:10.1016/j.biomaterials.2007.02.024.